Big-Data in Astronomy and Astrophysics

Extracting Meaning from Big-Data

Jason McEwen
www.jasonmcewen.org
@jasonmcewen

Mullard Space Science Laboratory (MSSL)
University College London (UCL)

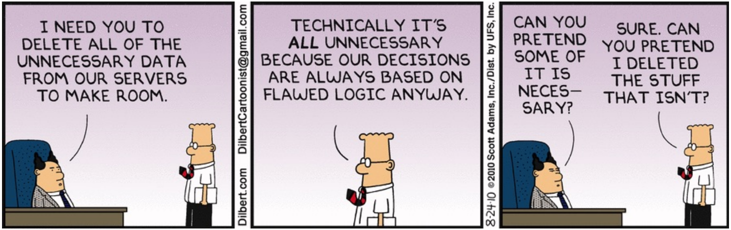

Connecting the Dots
Institute of High Energy Physics, Vienna, February 2016

Outline

1. Big-data in astronomy and astrophysics

2. Illustrative analyses
   - Planck
   - Euclid
   - LSST
   - SKA

3. Concluding remarks

What is big-data?

The nVs (originally 3Vs, then 6Vs, then 10Vs, . . .):

1. Volume: many bytes (e.g. typically peta, exabytes)
2. Variety: structural heterogeneity (e.g. sub-populations, variety of sources)
3. Velocity: rate of generation and analysis
4. Veracity: unreliability in sources
5. Variability: variation in data flow rate
6. Value: low value density
7. . . .

What is big-data?

The nVs (originally 3Vs, then 6Vs, then 10Vs, . . .):

1. Volume: many bytes (e.g. typically peta, exabytes)
2. Variety: structural heterogeneity (e.g. sub-populations, variety of sources)
3. Velocity: rate of generation and analysis
4. Veracity: unreliability in sources
5. Variability: variation in data flow rate
6. Value: low value density
7. . . .

What is big-data in astronomy and astrophysics?

- Big machines
  - experiments, physical hardware, computing
- Big theory and simulations for forward modelling
  - cosmological evolution of linear perturbations, N-body simulations, non-linear scales (astrophysics + cosmology), radiative transfer, semi-numerical methods
- Big parameter space
- Big algorithms
- Big collaborations
- Big engagement
  - *e.g.* outreach, industry

What is big-data in astronomy and astrophysics?

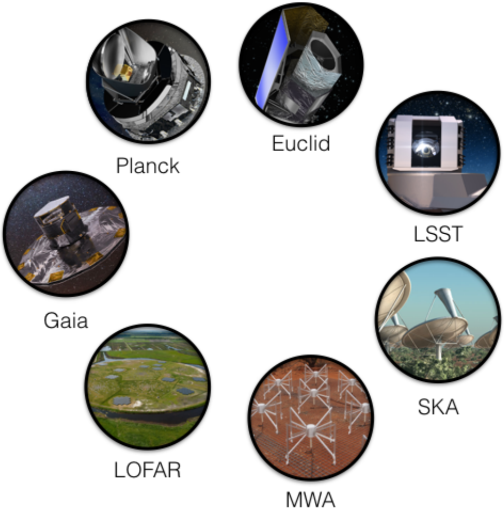

Wide and deep data and observations

Challenges of big-data

A. Gandomi, M. Haider / International Journal of Information Management 35 (2015) 137–144

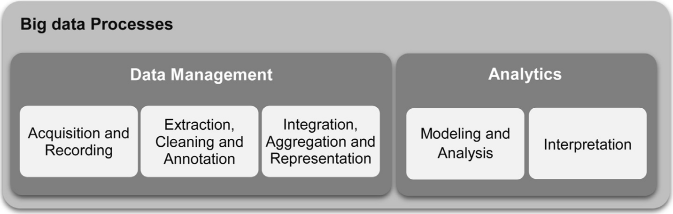

Fig. 3. Processes for extracting insights from big data.

Computational challenges:

- Data too big (to hold in memory)
- Access and analysis too slow (unfeasible)
- Too much power/energy required

Challenges of big-data

Analysis challenges (Fan et al. 2014):

1. Heterogeneity, e.g. sub-populations, different data sources, tension between data
2. Error accumulation, e.g. high-dimensional parameter spaces, bias
3. Spurious correlations, e.g. correlation vs causation, data dredging
4. Incident endogeneity, e.g. chance correlation between signal of interest and error

Challenges of big-data

Analysis challenges (Fan et al. 2014):

1. Heterogeneity, e.g. sub-populations, different data sources, tension between data
2. Error accumulation, e.g. high-dimensional parameter spaces, bias
3. Spurious correlations, e.g. correlation vs causation, data dredging
4. Incident endogeneity, e.g. chance correlation between signal of interest and error

Challenges of big-data

Analysis challenges (Fan et al. 2014):

1. Heterogeneity, e.g. sub-populations, different data sources, tension between data
2. Error accumulation, e.g. high-dimensional parameter spaces, bias
3. Spurious correlations, e.g. correlation vs causation, data dredging
4. Incident endogeneity, e.g. chance correlation between signal of interest and error

Challenges of big-data

Analysis challenges (Fan et al. 2014):

1. Heterogeneity, e.g. sub-populations, different data sources, tension between data
2. Error accumulation, e.g. high-dimensional parameter spaces, bias
3. Spurious correlations, e.g. correlation vs causation, data dredging
4. Incident endogeneity, e.g. chance correlation between signal of interest and error

Analysing big-data

Generic approaches to analysing big-data (Wang et al. 2015):

- Subsample
- Divide-and-conquer
- Stream processing

Additional approaches in astronomy and astrophysics:

- Exploit structure (geometry, symmetry, physics)
- Modelling:
  - Model-based consolidatory science
  - Model-agnostic exploratory science
- Approximation
- . . .

Analysing big-data

Generic approaches to analysing big-data (Wang et al. 2015):

- Subsample
- Divide-and-conquer
- Stream processing

Additional approaches in astronomy and astrophysics:

- Exploit structure (geometry, symmetry, physics)
- Modelling:
  - Model-based consolidatory science
  - Model-agnostic exploratory science
- Approximation
- ...

Analysing big-data

Examples of specific methods:

- Bayesian analysis
- MCMC sampling
- Hierarchical probabilistic (Bayesian) models
- Variable selection
- Experimental design
- Machine learning
- Optimisation
- Wavelets
- Sparsity
- Compressed sensing
- ...

$\Rightarrow$ Astrostatistics and Astroinformatics

Outline

1. Big-data in astronomy and astrophysics

2. Illustrative analyses
   - Planck
   - Euclid
   - LSST
   - SKA

3. Concluding remarks

ESA Planck satellite

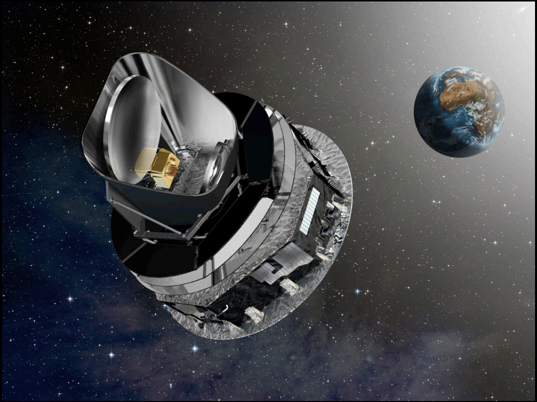

Credit: Planck

Observations made on the celestial sphere

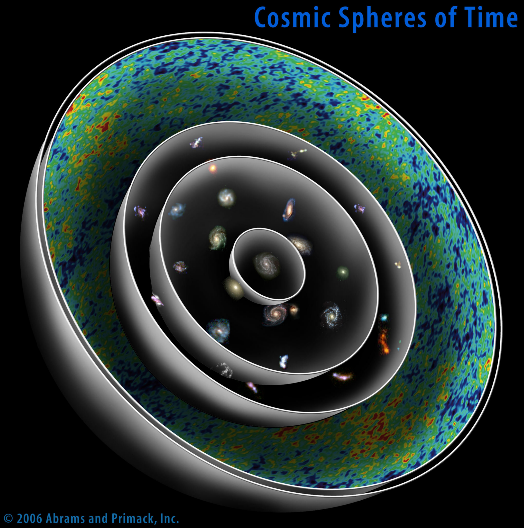

Observations of the cosmic microwave background (CMB)

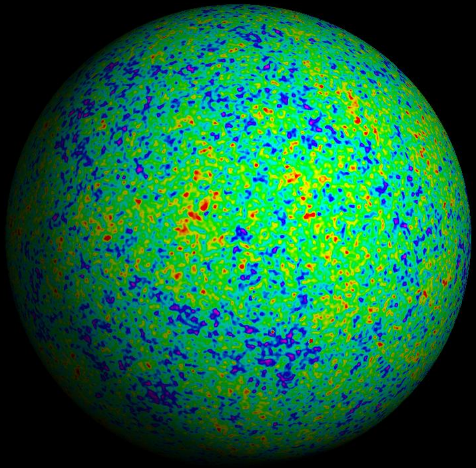

Credit: WMAP

Scale-discretised wavelets on the sphere
Transforms

- Spin scale-discretised wavelet transform is given by the projection onto each wavelet (Wiaux, McEwen *et al.* 2008, McEwen *et al.* 2013, McEwen *et al.* 2015):

$$\underbrace{\boxed{W^{{}_s\Psi^j}(\rho) = \langle {}_sf, \, \mathcal{R}_\rho \, {}_s\Psi^j \rangle}}_{\text{projection}} = \int_{\mathbb{S}^2} \mathrm{d}\Omega(\omega) \, {}_sf(\omega) (\mathcal{R}_\rho \, {}_s\Psi^j)^*(\omega) \, .$$

- Original function may be recovered exactly in practice from wavelet coefficients:

$${}_sf(\omega) = \underbrace{\boxed{\sum_{j=0}^{J}}}_{\text{finite sum}} \underbrace{\boxed{\int_{\mathrm{SO}(3)} \mathrm{d}\varrho(\rho) W^{{}_s\Psi^j}(\rho) (\mathcal{R}_\rho \, {}_s\Psi^j)(\omega) \, .}}_{\text{wavelet contribution}}$$

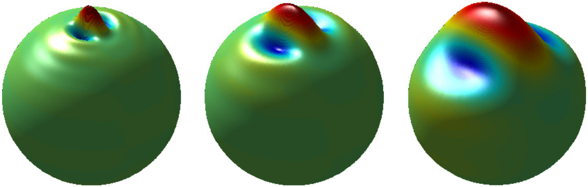

(a) $j = 4$ (b) $j = 3$ (c) $j = 2$

Figure: Scale-discretised wavelets on the sphere.

Scale-discretised wavelets on the sphere

Fast algorithms and codes

- Fast algorithms essential (McEwen, Leistedt *et al.* 2015, Leistedt, McEwen *et al.* 2013, McEwen *et al.* 2013, Leistedt McEwen *et al.* 2007, Wiaux, McEwen & Vielva 2007, Wiaux *et al.* 2005, Wandelt & Gorski 2001, Risbo 1996)

FastCSWT code

`http://www.fastcswt.org`

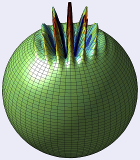

Fast directional continuous spherical wavelet transform algorithms

McEwen *et al.* (2007)

- Fortran
- Supports directional and steerable wavelets

S2DW code

`http://www.s2dw.org`

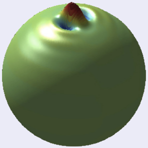

Exact reconstruction with directional wavelets on the sphere

Wiaux, McEwen, Vandergheynst, Blanc (2008)

- Fortran
- Parallelised
- Supports directional and steerable wavelets
- Supports inversion

Scale-discretised wavelets on the sphere

Fast algorithms and codes

S2LET code http://www.s2let.org

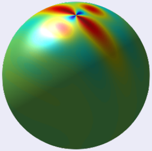

S2LET: Fast wavelet analysis on the sphere

McEwen, Leistedt, Büttner, Peiris & Wiaux (2015), Leistedt, McEwen, *et al.* (2012)

- C, Matlab, IDL, Python
- Supports directional and steerable wavelets, ridgelets and curvelets
- Supports inversion
- Supports spin
- Faster algorithms

SO3 code http://www.sothree.org

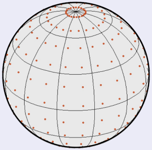

SO3: Fast Wigner transforms on the rotation group

McEwen, Büttner, Leistedt, Peiris & Wiaux (2015)

- C, Matlab, Python
- Fast and exact Fourier transforms on the rotation group $\mathrm{SO}(3)$

Planck component separation

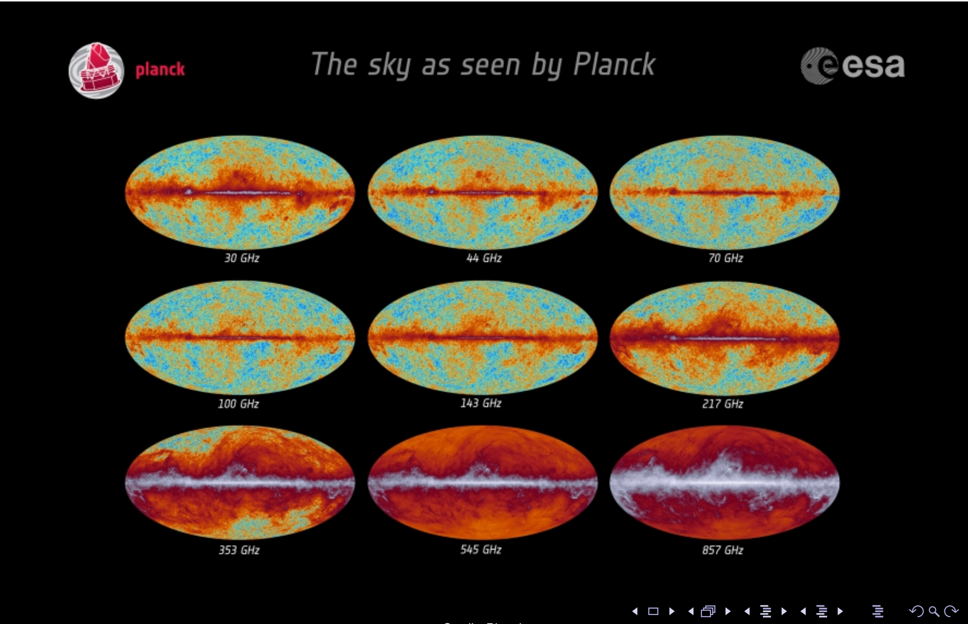

Planck component separation

SILC

- SILC: Blind Planck component separation via Scale-discretised, directional wavelet Internal Linear Combination (Rogers, Peiris, Leistedt, McEwen & Pontzen 2016)

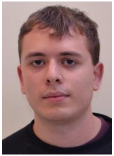

Keir Rogers

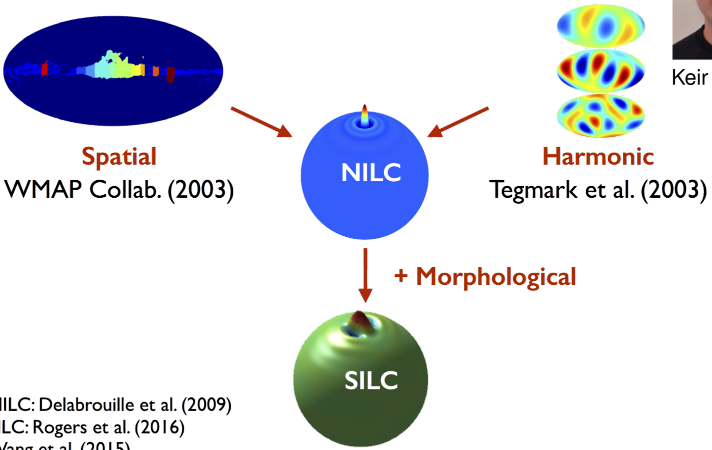

NILC: Delabrouille et al. (2009)
SILC: Rogers et al. (2016)
Wang et al. (2015)

Planck component separation
SILC

- SILC (R1) maps available for download: http://www.silc-cmb.org

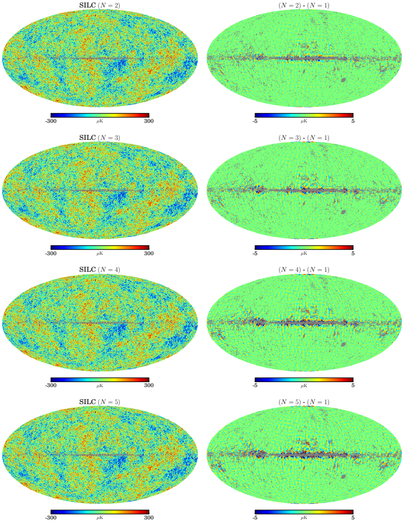

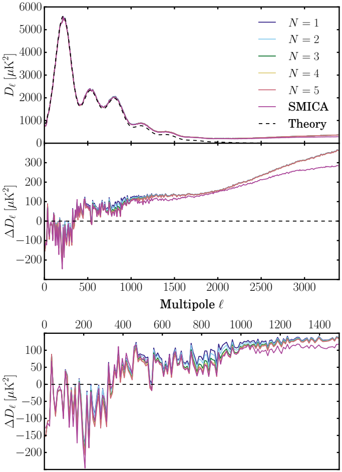

Bianchi VII$_h$ cosmologies

- Test fundamental assumptions on which modern cosmology is based, *e.g.* isotropy.
- Relax assumptions about the global structure of spacetime by allowing anisotropy about each point in the universe, *i.e.* rotation and shear.
- Yields more general solutions to Einstein's field equations $\rightarrow$ Bianchi cosmologies.
- Induces a characteristic subdominant, deterministic signature in the CMB, which is embedded in the usual stochastic anisotropies (Collins & Hawking 1973, Barrow *et al.* 1985).

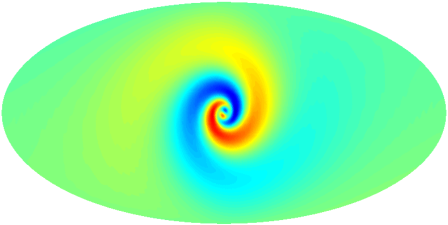

Figure: Bianchi CMB contribution.

Bianchi VII$_h$ cosmologies

Simulations

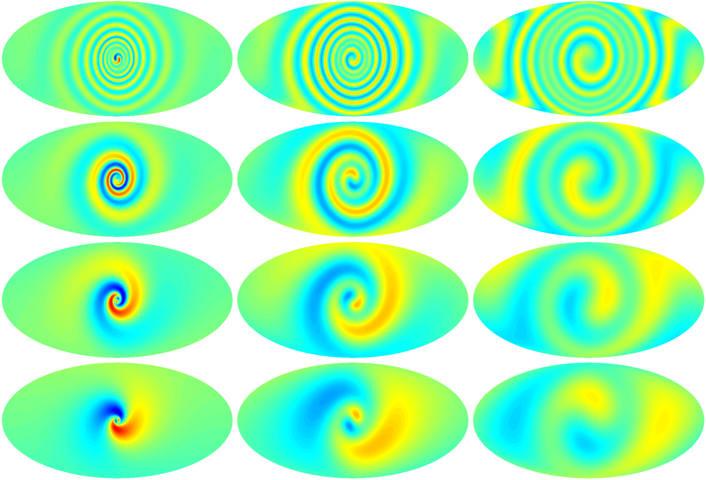

Figure: Simulated CMB contributions in Bianchi VII$_h$ cosmologies for varying parameters.

Bianchi VII$_h$ cosmologies
Bayesian analysis

- Apply Bayesian analysis of McEwen *et al.* (2013) to Planck data (previously WMAP).
- Likelihood given by

$$\boxed{\mathrm{P}(\boldsymbol{d} \mid \Theta_\mathrm{B}, \Theta_\mathrm{C}) \propto \frac{1}{\sqrt{|\mathbf{X}(\Theta_\mathrm{C})|}} \mathrm{e}^{\left[-\chi^2(\Theta_\mathrm{C},\Theta_\mathrm{B})/2\right]} ,}$$

where

$$\boxed{\chi^2(\Theta_\mathrm{C}, \Theta_\mathrm{B}) = \left[\boldsymbol{d} - \boldsymbol{b}(\Theta_\mathrm{B})\right]^\dagger \mathbf{X}^{-1}(\Theta_\mathrm{C}) \left[\boldsymbol{d} - \boldsymbol{b}(\Theta_\mathrm{B})\right] .}$$

- Compute the Bayesian evidence to determine preferred model:

$$\boxed{E = \mathrm{P}(\boldsymbol{d} \mid M) = \int \mathrm{d}\Theta \, \mathrm{P}(\boldsymbol{d} \mid \Theta, M) \, \mathrm{P}(\Theta \mid M) .}$$

- Use MultiNest to compute the posteriors and evidences via nested sampling (Feroz & Hobson 2008, Feroz *et al.* 2009).

Bianchi VII$_h$ cosmologies

Planck component-separated data

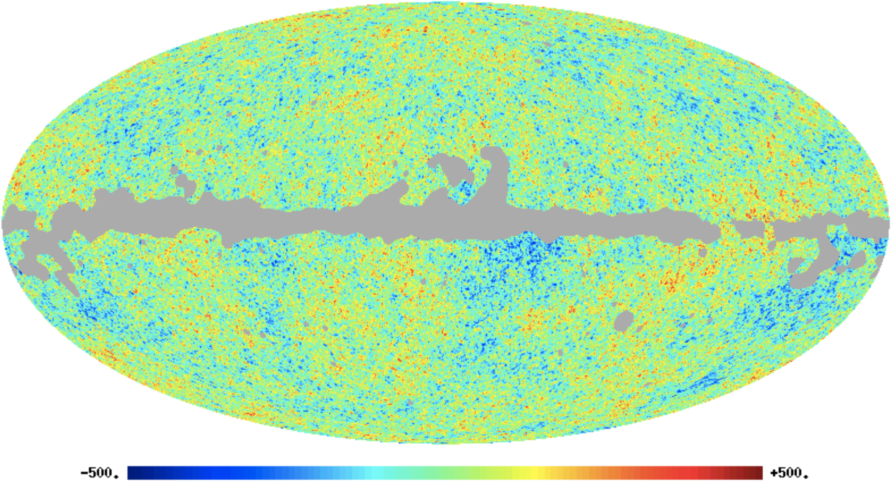

Figure: *Planck* 2013 `SMICA` component-separated data.

Bianchi VII$_h$ cosmologies

Best-fit Bianchi component (flat-decoupled-Bianchi model)

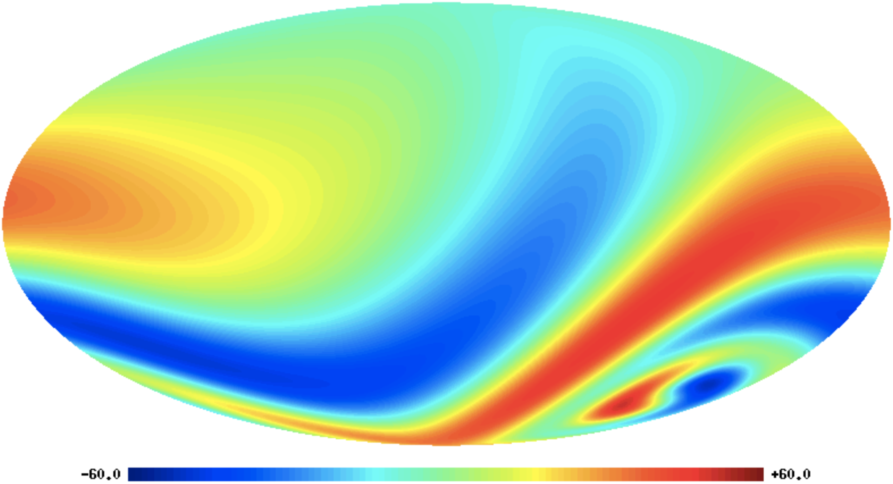

Figure: Best-fit template of flat-decoupled-Bianchi VII$_h$ model.

Bianchi VII$_h$ cosmologies
Planck results

BUT parameter estimates are not consistent with concordance cosmology.

- Follow up with Planck 2015 polarisation data, rules our flat-Bianchi-decoupled model.
- Find no evidence for Bianchi VII$_h$ cosmologies and constrain vorticity to (Planck Collaboration XVIII 2015):

$$\boxed{(\omega/H)_0 < 7.6 \times 10^{-10}}$$

95% confidence level

Outline

1. Big-data in astronomy and astrophysics

2. Illustrative analyses
   - Planck
   - Euclid
   - LSST
   - SKA

3. Concluding remarks

ESA Euclid satellite

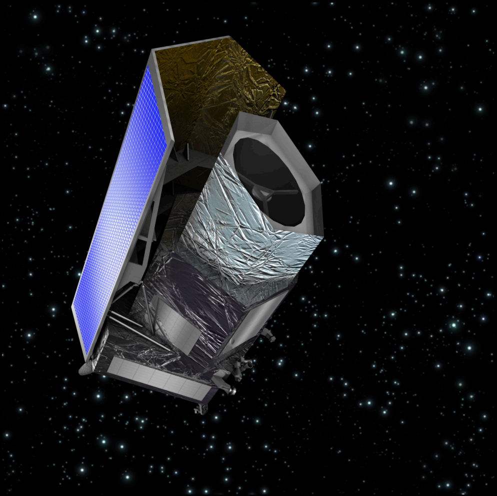

Credit: Euclid

Euclid sky coverage

Switch on

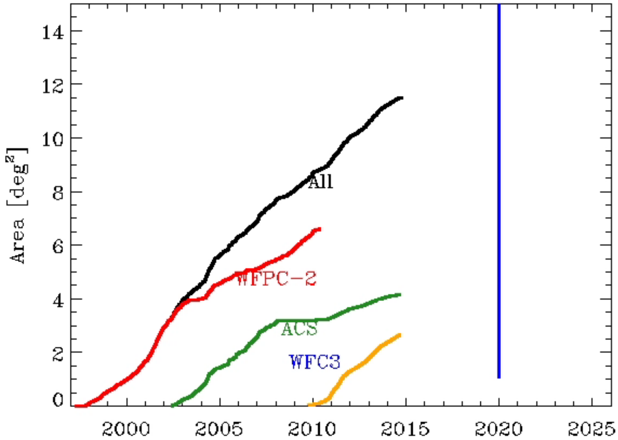

Credit: Tom Kitching

Euclid sky coverage

2 weeks

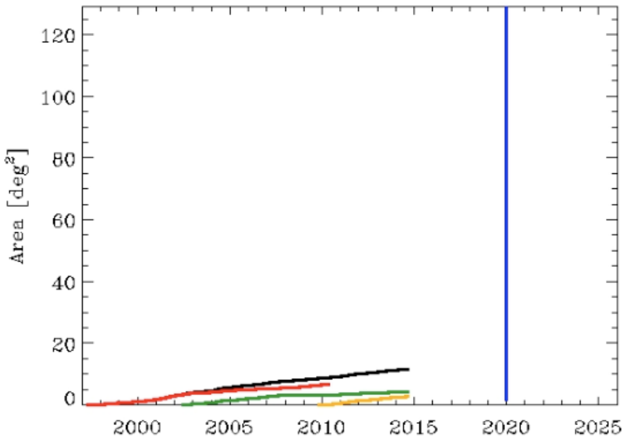

Credit: Tom Kitching

Euclid sky coverage

6 months

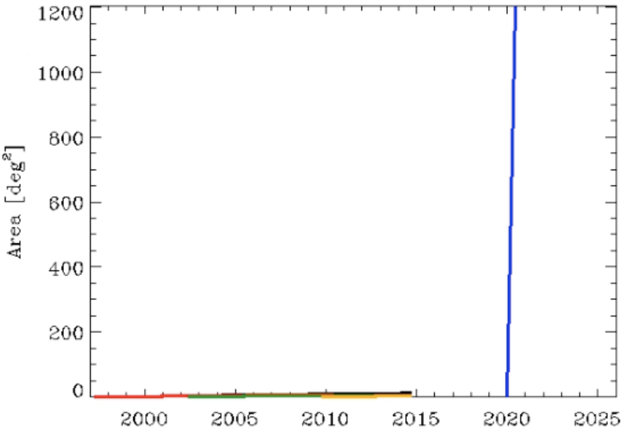

Credit: Tom Kitching

Euclid sky coverage

1 year

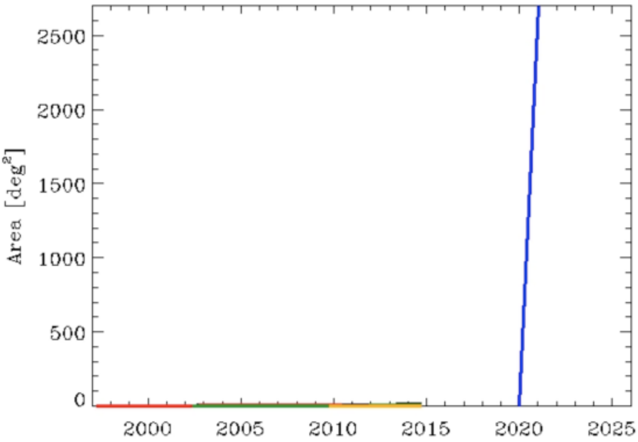

Credit: Tom Kitching

Euclid sky coverage

5 years

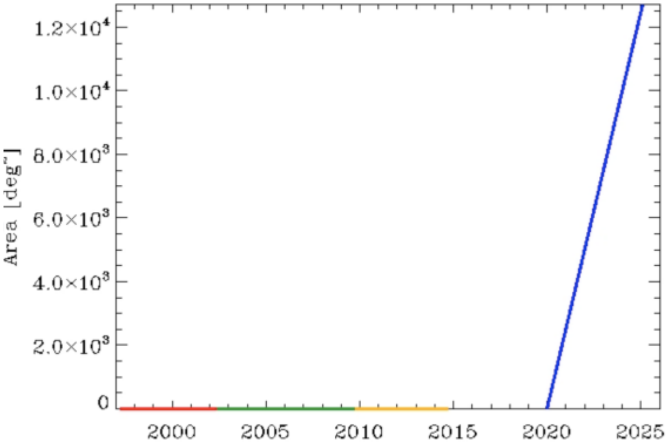

Credit: Tom Kitching

Galaxies on the 3D ball

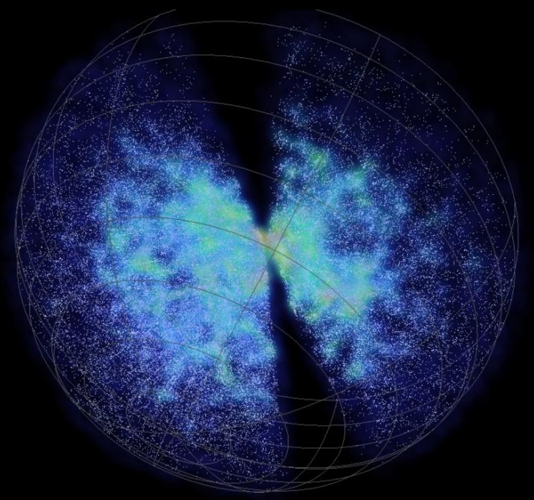

Credit: SDSS

Fourier-LAGuerre wavelets (flaglets) on the ball

- Fourier-Laguerre wavelet (flaglet) transform is given by the projection onto each wavelet (Leistedt & McEwen 2012):

$$\underbrace{\boxed{W^{{}_s\Psi^{jj'}}(r,\rho) = \langle {}_s f,\ \mathcal{T}_{(r,\rho)}\ {}_s\Psi^{jj'}\rangle}}_{\text{projection}} = \int_{\mathbb{B}^3} \mathrm{d}^3\boldsymbol{r}\ {}_s f(\boldsymbol{r}) (\mathcal{T}_{(r,\rho)}\ {}_s\Psi^{jj'})^*(\boldsymbol{r})\ .$$

- Original function may be recovered exactly in practice from wavelet coefficients:

$${}_s f(\boldsymbol{r}) = \underbrace{\boxed{\sum_{jj'}}}_{\text{finite sum}} \underbrace{\boxed{\int_{\mathrm{SO}(3)} \mathrm{d}\varrho(\rho) \int_{\mathbb{R}+} \mathrm{d}r\, W^{{}_s\Psi^{jj'}}(r,\rho) (\mathcal{T}_{(r,\rho)}\ {}_s\Psi^{jj'})(\boldsymbol{r})\ .}}_{\text{wavelet contribution}}$$

Fourier-LAGuerre wavelets (flaglets) on the ball

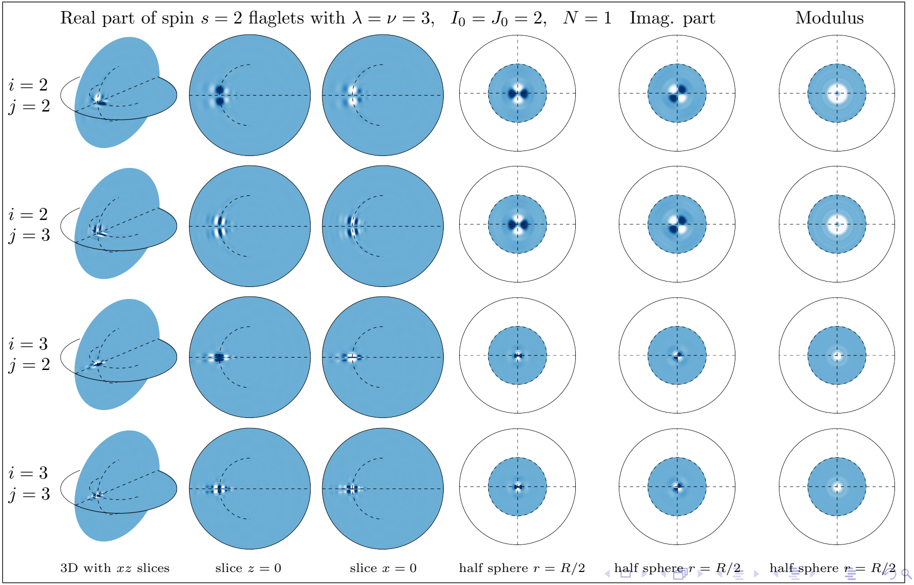

3D weak gravitational lensing

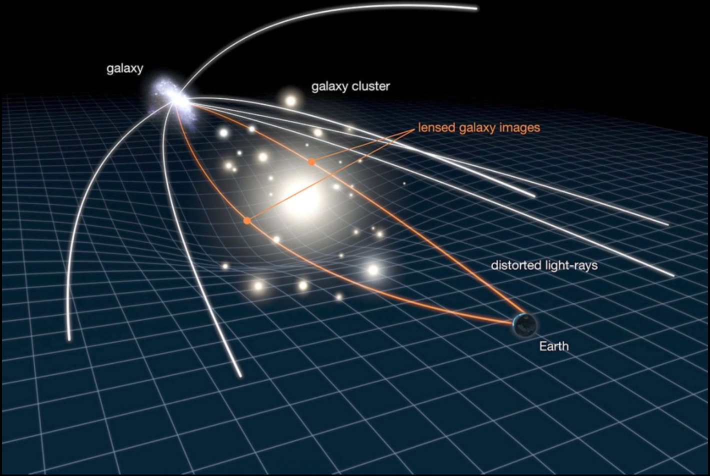

Credit: CFHTLenS

3D weak gravitational lensing

- 3D weak lensing with spin wavelets on the ball (Leistedt, McEwen, Kitching, Peiris 2015).

- Wavelet transform of 3D cosmic shear:

$$\boxed{W_{2\gamma}^{2\Psi^{ij}}(\boldsymbol{n}, r) = ({}_2\gamma \odot {}_2\Psi^{ij})(\boldsymbol{n}, r)}$$

- Wavelet covariance:

$$\boxed{C^{ij,i'j'}(\boldsymbol{n}, \boldsymbol{n}', r, r') = \langle\, W_{2\gamma}^{2\Psi^{ij}}(\boldsymbol{n}, r)\; W_{2\gamma}^{2\Psi^{i'j'}\,*}(\boldsymbol{n}', r')\,\rangle}$$

compute from data

- Theory wavelet covariance:

$$\boxed{C^{ij,i'j'}(\boldsymbol{n}\cdot\boldsymbol{n}', r, r') \;=\; \frac{2}{\pi}\sum_{\ell}\frac{(N_{\ell,2})^2}{4}\int_{\mathbb{R}+}\mathrm{d}k k^2\int_{\mathbb{R}+}\mathrm{d}k' k'^2\; C_\ell^{\phi\phi}(k,k')\; P_\ell(\boldsymbol{n}\cdot\boldsymbol{n}')\; {}_2\mathcal{H}_\ell^{ij}(k,r)\; {}_2\mathcal{H}_\ell^{i'j'\,*}(k',r')}$$

compute from theory

- Simultaneous spatial and scale representation (can handle complicated sky coverage and filter unreliable harmonic modes).

Boris Leistedt

Outline

1. Big-data in astronomy and astrophysics

2. Illustrative analyses
   - Planck
   - Euclid
   - LSST
   - SKA

3. Concluding remarks

Large Synoptic Survey Telescope (LSST)

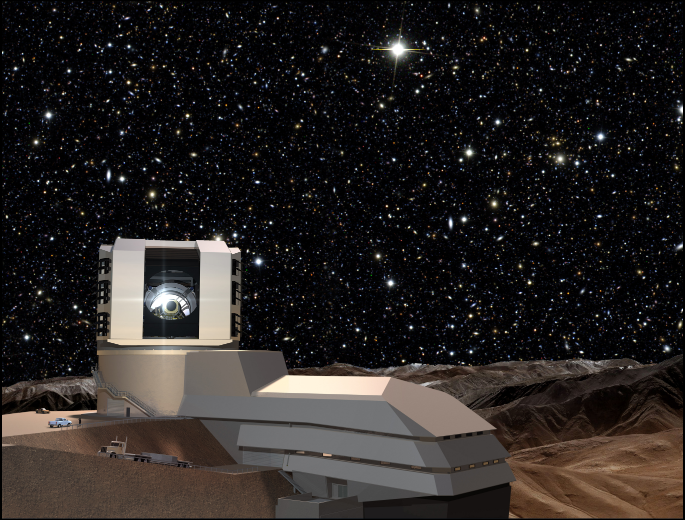

Credit: LSST

Supernova

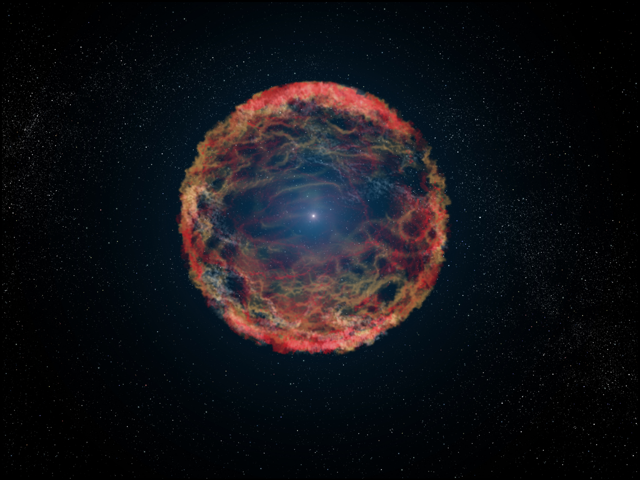

Credit: SpaceTelescope.org

Photometric supernova classification

Machine learning

- Photometric supernova classification by machine learning (Lochner, McEwen, Peiris & Lahav, in prep.)
- Go beyond single techniques to study classes.
- Understand physical requirements (*e.g.* representative training, redshift).

Michelle Lochner

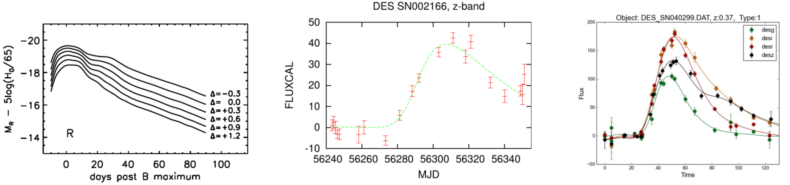

(a) Templates (b) Generic parameterisations (c) Wavelets (non-parametric)

Figure: Feature selection classes (in order of increasing model independence)

Photometric supernova classification

Importance of representative training data

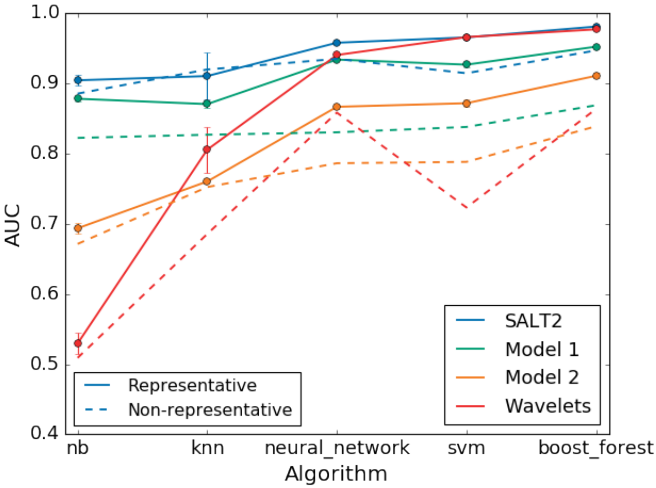

Photometric supernova classification

Importance of redshift

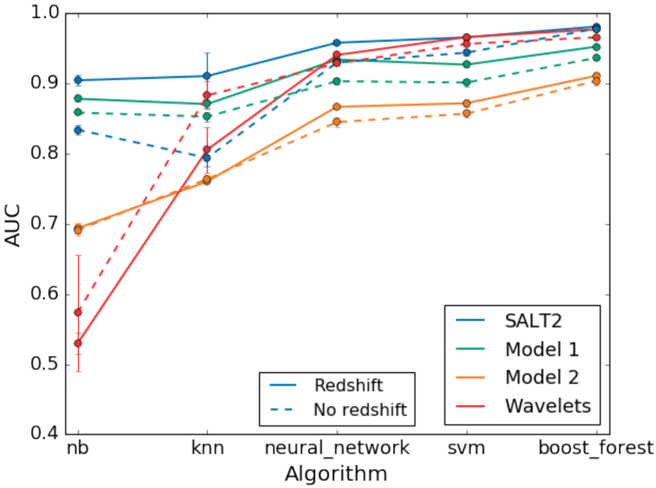

Outline

1. Big-data in astronomy and astrophysics

2. Illustrative analyses
   - Planck
   - Euclid
   - LSST
   - SKA

3. Concluding remarks

Square Kilometre Array (SKA)

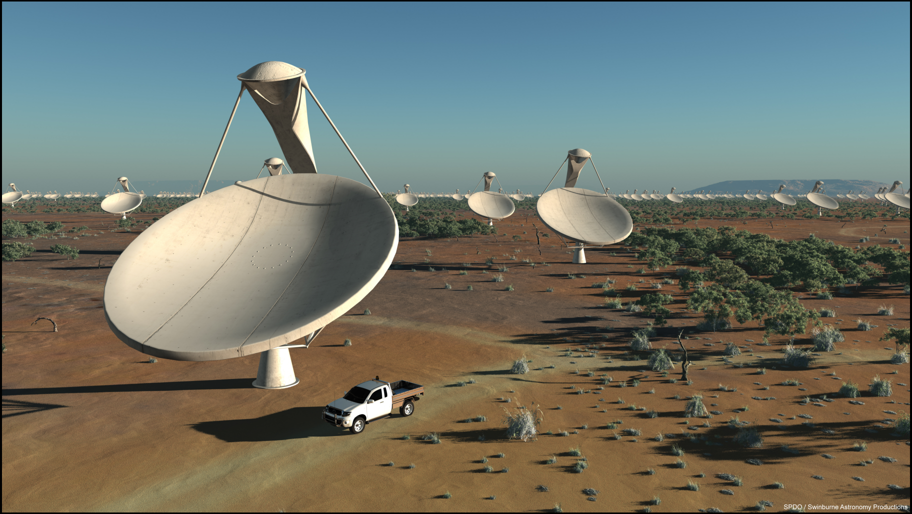

Credit: SKA

SKA sites

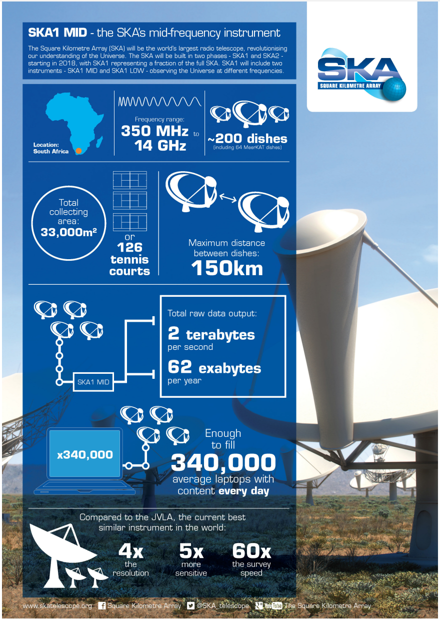
SKA1 MID - the SKA's mid-frequency instrument
The Square Kilometre Array (SKA) will be the world's largest radio telescope, revolutionising our understanding of the Universe. The SKA will be built in two phases - SKA1 and SKA2 - starting in 2018, with SKA1 representing a fraction of the full SKA. SKA1 will include two instruments - SKA1 MID and SKA1 LOW - observing the Universe at different frequencies.
SKA SQUARE KILOMETRE ARRAY
Location: South Africa
Frequency range:
350 MHz to 14 GHz
~200 dishes
(including 64 MeerKAT dishes)
Total collecting area: 33,000m²
or 126 tennis courts
Maximum distance between dishes: 150km
SKA1 MID
Total raw data output:
2 terabytes per second
62 exabytes per year
x340,000
Enough to fill 340,000 average laptops with content every day
Compared to the JVLA, the current best similar instrument in the world:
4x the resolution
5x more sensitive
60x the survey speed
www.skatelescope.org Square Kilometre Array @SKA_telescope The Square Kilometre Array

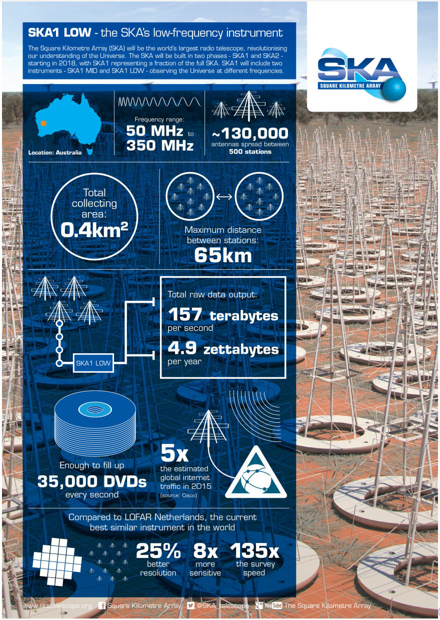
SKA1 LOW - the SKA's low-frequency instrument
The Square Kilometre Array (SKA) will be the world's largest radio telescope, revolutionising our understanding of the Universe. The SKA will be built in two phases - SKA1 and SKA2 - starting in 2018, with SKA1 representing a fraction of the full SKA. SKA1 will include two instruments - SKA1 MID and SKA1 LOW - observing the Universe at different frequencies.
SKA SQUARE KILOMETRE ARRAY
Location: Australia
Frequency range:
50 MHz to 350 MHz
~130,000 antennas spread between 500 stations
Total collecting area: 0.4km²
Maximum distance between stations: 65km
SKA1 LOW
Total raw data output:
157 terabytes per second
4.9 zettabytes per year
Enough to fill up 35,000 DVDs every second
5x the estimated global internet traffic in 2015
(source: Cisco)
Compared to LOFAR Netherlands, the current best similar instrument in the world
25% better resolution
8x more sensitive
135x the survey speed
www.skatelescope.org Square Kilometre Array @SKA_telescope The Square Kilometre Array

The SKA poses a considerable big-data challenge

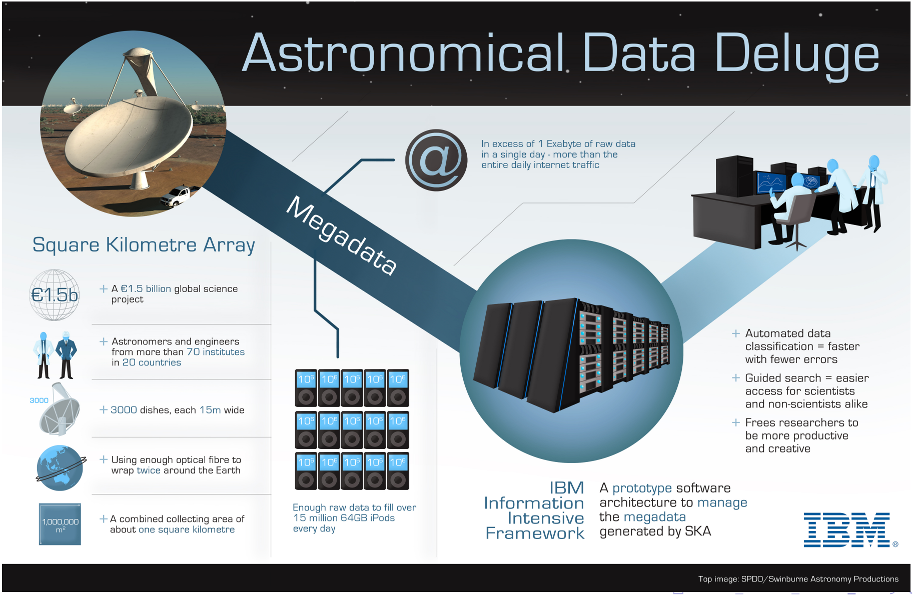

The SKA poses a considerable big-data challenge

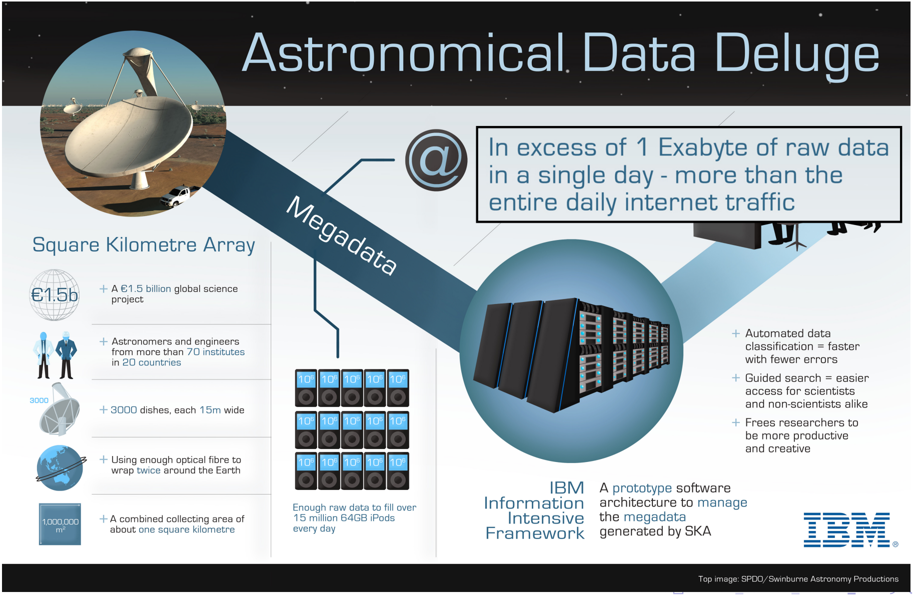

Radio interferometric telescopes acquire “Fourier” measurements

“Fourier” Measurements

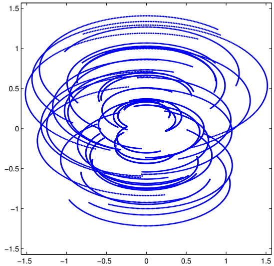

Compressive sensing

- Developed by Candes *et al.* 2006 and Donoho 2006 (and others).
- Although many underlying ideas around for a long time.
- Exploits the sparsity of natural signals.
- Next evolution of wavelet analysis.
- Acquisition versus imaging.

(a) Emmanuel Candes

(b) David Donoho

Radio interferometric inverse problem

- Consider the ill-posed inverse problem of radio interferometric imaging:

$$\boxed{\boldsymbol{y} = \Phi \boldsymbol{x} + \boldsymbol{n}} \,,$$

where $\boldsymbol{y}$ are the measured visibilities, Φ is the linear measurement operator, $\boldsymbol{x}$ is the underlying image and $\boldsymbol{n}$ is instrumental noise.

- Measurement operator $\boxed{\Phi = \mathbf{M}\,\mathbf{F}\,\mathbf{C}\,\mathbf{A}}$ may incorporate:
  - primary beam $\mathbf{A}$ of the telescope;
  - w-modulation modulation $\mathbf{C}$;
  - Fourier transform $\mathbf{F}$;
  - masking $\mathbf{M}$ which encodes the incomplete measurements taken by the interferometer.

Radio interferometric inverse problem

- Consider the ill-posed inverse problem of radio interferometric imaging:

$$\boxed{\boldsymbol{y} = \Phi \boldsymbol{x} + \boldsymbol{n}}\,,$$

where $\boldsymbol{y}$ are the measured visibilities, Φ is the linear measurement operator, $\boldsymbol{x}$ is the underlying image and $\boldsymbol{n}$ is instrumental noise.

- Measurement operator $\boxed{\Phi = \mathbf{M}\,\mathbf{F}\,\mathbf{C}\,\mathbf{A}}$ may incorporate:
  - primary beam $\mathbf{A}$ of the telescope;
  - w-modulation modulation $\mathbf{C}$;
  - Fourier transform $\mathbf{F}$;
  - masking $\mathbf{M}$ which encodes the incomplete measurements taken by the interferometer.

Radio interferometric inverse problem

- Consider the ill-posed inverse problem of radio interferometric imaging:

$$\boxed{\boldsymbol{y} = \Phi \boldsymbol{x} + \boldsymbol{n}} \, ,$$

where $\boldsymbol{y}$ are the measured visibilities, Φ is the linear measurement operator, $\boldsymbol{x}$ is the underlying image and $\boldsymbol{n}$ is instrumental noise.

- Measurement operator $\boxed{\Phi = \mathbf{M}\,\mathbf{F}\,\mathbf{C}\,\mathbf{A}}$ may incorporate:
  - primary beam $\mathbf{A}$ of the telescope;
  - w-modulation modulation $\mathbf{C}$;
  - Fourier transform $\mathbf{F}$;
  - masking $\mathbf{M}$ which encodes the incomplete measurements taken by the interferometer.

Interferometric imaging: recover an image from noisy and incomplete Fourier measurements.

Interferometric imaging with compressed sensing

- Solve the interferometric imaging problem

$$\boxed{\boldsymbol{y} = \Phi \boldsymbol{x} + \boldsymbol{n} \quad \text{with} \quad \Phi = \mathbf{M}\,\mathbf{F}\,\mathbf{C}\,\mathbf{A}} \,,$$

- Leverage ideas from compressive sensing (Donoho, Candes) by applying a prior on sparsity of the signal in a sparsifying dictionary Ψ.
- Basis Pursuit (BP) denoising problem

$$\boxed{\boldsymbol{\alpha}^\star = \underset{\boldsymbol{\alpha}}{\arg\min} \|\boldsymbol{\alpha}\|_1 \;\text{ such that }\; \|\boldsymbol{y} - \Phi\Psi\boldsymbol{\alpha}\|_2 \leq \epsilon \,,} \quad \text{BPDN}$$

where the image is synthesised by $\boldsymbol{x}^\star = \Psi\boldsymbol{\alpha}^\star$.

Interferometric imaging with compressed sensing

- Solve the interferometric imaging problem

$$\boxed{\boldsymbol{y} = \Phi \boldsymbol{x} + \boldsymbol{n} \quad \text{with} \quad \Phi = \mathbf{M}\,\mathbf{F}\,\mathbf{C}\,\mathbf{A}},$$

- Leverage ideas from compressive sensing (Donoho, Candes) by applying a prior on sparsity of the signal in a sparsifying dictionary Ψ.

- Basis Pursuit (BP) denoising problem

$$\boxed{\boldsymbol{\alpha}^\star = \underset{\boldsymbol{\alpha}}{\arg\min} \|\alpha\|_1 \quad \text{such that} \quad \|\boldsymbol{y} - \Phi\Psi\boldsymbol{\alpha}\|_2 \leq \epsilon\,,} \; \text{BPDN}$$

where the image is synthesised by $\boldsymbol{x}^\star = \Psi\boldsymbol{\alpha}^\star$.

SARA for radio interferometric imaging

Algorithm

- Sparsity averaging reweighted analysis (SARA) for RI imaging (Carrillo, McEwen & Wiaux 2012)

- Consider a dictionary composed of a concatenation of orthonormal bases, i.e.

$$\boxed{\Psi = \frac{1}{\sqrt{q}}[\Psi_1, \Psi_2, \ldots, \Psi_q],}$$

  thus $\Psi \in \mathbb{R}^{N\times D}$ with $D = qN$.

- We consider the following bases: Dirac (*i.e.* pixel basis); Haar wavelets (promotes gradient sparsity); Daubechies wavelet bases two to eight.
  $\Rightarrow$ concatenation of 9 bases

- Promote average sparsity by solving the reweighted ℓ_1 analysis problem:

$$\boxed{\min_{\bar{\boldsymbol{x}}\in\mathbb{R}^N} \|W\Psi^T\bar{\boldsymbol{x}}\|_1 \quad \text{subject to} \quad \|\boldsymbol{y} - \Phi\bar{\boldsymbol{x}}\|_2 \leq \epsilon \quad \text{and} \quad \bar{\boldsymbol{x}} \geq 0\,,} \quad \text{SARA}$$

  where $W \in \mathbb{R}^{D\times D}$ is a diagonal matrix with positive weights.

- Solve a sequence of reweighted ℓ_1 problems using the solution of the previous problem as the inverse weights $\rightarrow$ approximate the ℓ_0 problem.

SARA for radio interferometric imaging

Results on simulations

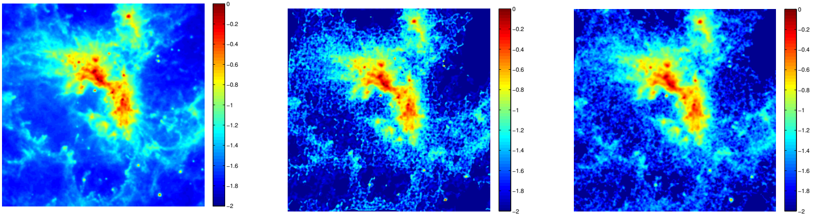

(a) Original (b) “CLEAN” (SNR=16.67 dB) (c) “MS-CLEAN” (SNR=17.87 dB)

SARA for radio interferometric imaging

Results on simulations

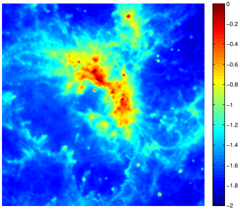

(a) Original

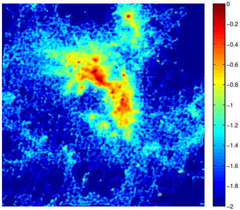

(b) “CLEAN” (SNR=16.67 dB)

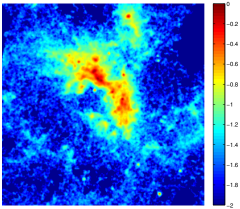

(c) “MS-CLEAN” (SNR=17.87 dB)

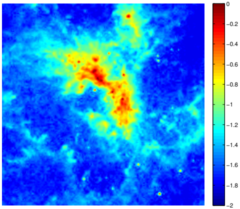

(d) BPDb8 (SNR=24.53 dB)

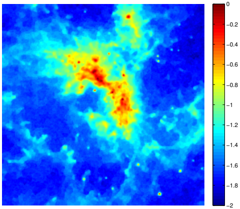

(e) TV (SNR=26.47 dB)

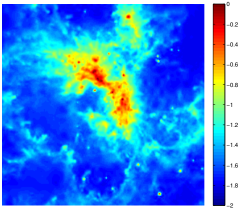

(f) SARA (SNR=29.08 dB)

Supporting continuous visibilities

Results on simulations

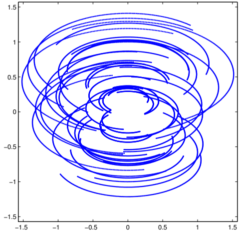

(a) Coverage

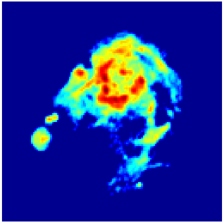

(b) M31 (ground truth)

Figure: Reconstructed images from continuous visibilities.

Supporting continuous visibilities

Results on simulations

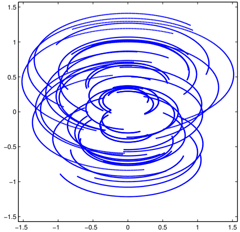

(a) Coverage

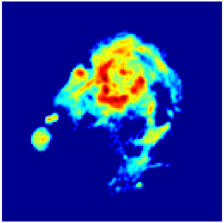

(b) M31 (ground truth)

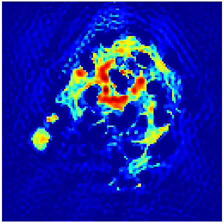

(c) "CLEAN" (SNR= 8.2dB)

Figure: Reconstructed images from continuous visibilities.

Supporting continuous visibilities

Results on simulations

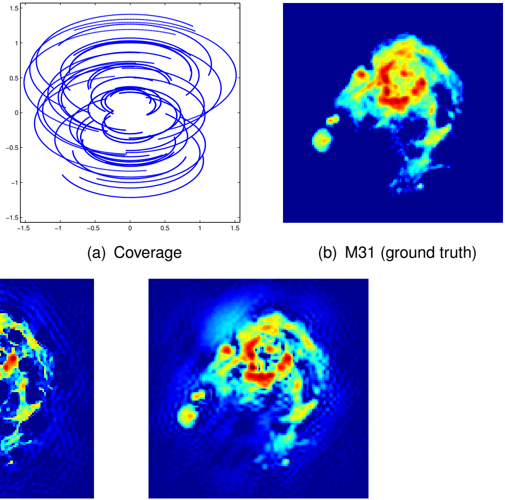

(a) Coverage

(b) M31 (ground truth)

(c) "CLEAN" (SNR= 8.2dB)

(d) "MS-CLEAN" (SNR= 11.1dB)

Figure: Reconstructed images from continuous visibilities.

Supporting continuous visibilities

Results on simulations

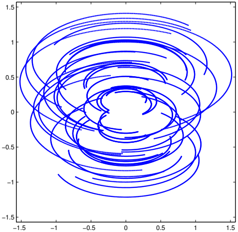

(a) Coverage

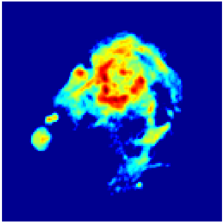

(b) M31 (ground truth)

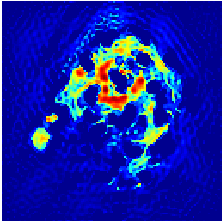

(c) “CLEAN” (SNR= 8.2dB)

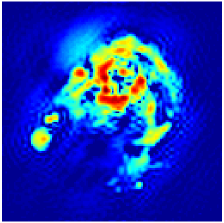

(d) “MS-CLEAN” (SNR= 11.1dB)

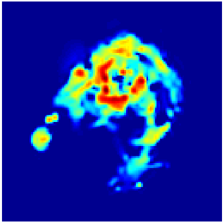

(e) SARA (SNR= 13.4dB)

Figure: Reconstructed images from continuous visibilities.

Distributed algorithms and codes

- Distributed storage and computation (Onose *et al.* 2016) by divide-and-conquer and sub-sampling techniques

SOPT code http://basp-group.github.io/sopt/

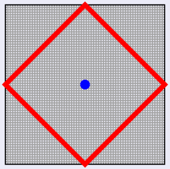

Sparse OPTimisation
Carrillo, McEwen, Wiaux

SOPT is an open-source code that provides functionality to perform sparse optimisation using state-of-the-art convex optimisation algorithms.

PURIFY code http://basp-group.github.io/purify/

Next-generation radio interferometric imaging
Carrillo, McEwen, Wiaux

PURIFY is an open-source code that provides functionality to perform radio interferometric imaging, leveraging recent developments in the field of compressive sensing and convex optimisation.

Concluding remarks

- Increasingly inter-disciplinary, drawing on statistics, applied mathematics, computer science, information engineering, ...
- Increasingly intra-disciplinary (*e.g.* Planck, Euclid, LSST, SKA, ...)
- Many methodological synergies

Concluding remarks

How can we exploit synergies?

1. Open (unencumbered) data and open code
2. Develop best practices (*e.g.* code development, general codes, reproducible/replicable research, blinded analysis)
3. Explore HPC synergies (*e.g.* Dirac, Archer, Hartree, Google, Amazon, . . .)
4. Go beyond individual techniques to understand properties of classes of approach
5. Develop common language
6. Promote inter- and intra-disciplinary collaboration and communication, *e.g.* Alan Turing Institute (ATI), workshops (*e.g.* BASP conference), Hackathons, . . .
7. . . .